Caesium and tungsten behaviour in the filamented arc driven Kamaboko-III negative ion source

Caesium and tungsten behaviour in the filamented arc driven Kamaboko-III negative ion source

A. Krylov[1,6]**, D. Boilson**[2]**, U. Fantz**[3]**, R.S. Hemsworth**[4]**, O. Provitina**[4]**, S. Pontremoli**[4] **and B. Zaniol**[5]

[1] RRC 'Kurchatov Institute', pl. Kurchatova 1, Moscow 123182, Russia

[2] Association EURATOM-DCU, PRL/NCPST, Glasnevin, Dublin 13, Ireland

[3] Max-Planck-Institut für Plasmaphysik, EURATOM Association, Postfach 1533, D-85740 Garching, Germany

[4] Association EURATOM-CEA, CEA Cadarache, F-13108, St. Paul lez Durance, France

[5] CONSORZIO RFX Association EURATOM-ENEA, Corso Stati Uniti 4, I-35127 Padova, Italy

E-mail: krylov@fusion.ru

Abstract

The ITER neutral beam injection is based on the acceleration and neutralization of negative deuterium ions. The target performance for the ITER beam source is to accelerate to 1 MeV a 40 A D$^-$ beam, with a current density of 200 A m^{-2}, with pulse lengths of $\geqslant$1000 s. It was found that in long pulse operation the negative ion yield from the filamented Kamaboko III ion source (a model of ITER ion source) degrades in comparison with short pulse operation, <5 s. This could be linked to the behaviour of caesium (Cs), which is added to the source to increase its negative ion yield and tungsten (W) evaporated from filaments. Cs and W are co-adsorbed on the source walls and the plasma grid and the composition of this coating can vary during long pulse operation. The possible consequences of this changing surface on the negative ion production will be discussed.

Tungsten filaments have a limited lifetime in the ion source and changing filaments and refilling of the Cs oven are the only scheduled maintenance events for the ITER injectors. These are complicated operations as the ITER injectors will be highly activated and all maintenance has to be carried out remotely. Therefore, increasing the filament lifetime and decreasing the Cs consumption are highly desirable. This paper presents results of relative measurements (including spectroscopic and chemical) of the W content of the Kamaboko-III source and reports relevant calculations on Cs consumption and W evaporation.

PACS numbers: 52.50.Dg, 52.25.Jm, 52.70.Kz

(Some figures in this article are in colour only in the electronic version)

1. Introduction

In pure hydrogen discharges operated with 0.3 Pa filling pressure, the Kamaboko III filamented arc driven negative ion source can provide, typically, extracted current densities of 2–3 mA cm^{-2} of H$^-$ ions at a discharge power of $\approx$45 kW. It has been widely demonstrated that operation of such a source with Cs seeding allows the production of negative ions by surface production, which increases the negative ion yield up to $\approx$10–12 mA cm^{-2}, at the same discharge power [1–3]. This is referred to as the 'Cs effect'. It has also been demonstrated

in short pulses (up to 5 s) that increasing the plasma grid (PG) temperature to approximately 230–300 °C can enhance the negative ion yield by a factor of 2–3 [2, 4]; this effect is referred to as the 'PG temperature effect'. Combining these effects should allow the ITER required 20–25 mA cm^{-2} to be achieved.

However, in a number of long pulse experiments [5, 6] carried out on the MANTIS test bed, at the DRFC, CEA Cadarache, it has been found that both effects are not as pronounced as expected. In short pulse operation, with Cs seeding, high accelerated negative ion densities have been achieved, but the efficiency of the beam source degrades over

[6] Author to whom any correspondence should be addressed.

Table 1. Surface coverage in the Kamaboko III ion source.

	Cs	W	Cu	Ca	Mo	Fe	Al
Mass (mg) in the area indicated. First row is from the solution, the second from the sediment							
PG extraction area	150	58.5	1.2	6.3	2.7	—	—
	2.84	76.9	12	3.06	0.189	0.473	3.42
PG periphery (frame)[b]	2400	310	3	21	8	—	—
	7.58	15.6	32.5	1.86	0.031	0.162	1.47
Arc chamber walls	6000	1250	8	7	30	—	—
	13.8	46.6	18.2	2.82	0.123	0.159	0.246
Total (g)	8.6	1.8	0.07	0.04	0.04	0.001	0.005
Surface density in the area indicated (atom/cm^2)							
PG extraction	2.5E + 18	1.6E + 18	4.5E + 17	5.1E + 17	6.6E + 16	1.8E + 16	2.8E + 17
PG periphery	1.3E + 19	1.3E + 18	4.0E + 17	4.1E + 17	5.9E + 16	2.1E + 15	3.9E + 16
Arc chamber	4.9E + 18	7.5E + 17	4.4E + 16	2.6E + 16	3.3E + 16	3.0E + 14	9.6E + 14

[a] Traces of Cr, Na, Mg and Si were also found.
[b] For this campaign there were no side masks on the PG. (The side masks are shown in figure 1).

a number of days. By adding new Cs or continuous injecting Cs, the optimal conditions can be re-achieved.

The Cs effect is assumed to arise due to the reduction of the work function value of the clean metal surface (4–5 eV) to $\varphi_{Cs} = 1.81$ eV when covered with Cs, allowing conditions for the production of surface created negative ions. The PG temperature effect could be explained as being due to evaporation of the excess Cs with increased temperature of the PG, from $\theta_{Cs} > 1$, where $\theta_{Cs} = 1$ corresponds to one mono-layer, to sub-monolayer coverage, which results in a work function in the range

$$\varphi(\theta_{Cs} \geqslant 1) = 1.81\,\text{eV} \geqslant \varphi(\theta_{Cs}) > \varphi_{\min}(\theta_{Cs} \approx 0.6) = 1.45\,\text{eV}.$$

for the 'ideal' case of Cs sub-monolayer coverage on (110) W crystal surface. From data in [1], the PG temperature effect could be as large as 530%.

The observed reduction in the PG temperature effect in long pulse operation led to the suggestion that the relatively high equilibrium temperature of the ion source walls achieved in long pulses (70–90 °C) could lead to a high evaporation rate of Cs from the source walls, leading to a thick ($\theta_{Cs} \geqslant 1$) layer on the PG even when the PG is at the 'prescribed' temperature of ≈ 300 °C. The rapid decline in the basic Cs effect led to the suggestion that Cs could be lost from the source due to the high evaporation from the walls, hence a high Cs flux out through the apertures in the PG. However, chemical analyses of the layers on the source walls after extended periods of operation indicate that the bulk of the injected Cs was still inside the arc, see table 1 and [3]. Tungsten is evaporated from the filaments and it is suggested, that the Cs is 'blocked' [7] on the walls in a loosely bound tungsten–caesium mixture.

2. Fluxes in the beam source

In a filamented arc driven negative ion source we can identify several fluxes of particles that are of importance for the negative ion production and extraction. These are the following.

2.1. Hydrogen gas flow to the arc chamber

Ideally a negative ion source is operated at as low pressure as possible in order to minimize the gas flow from the source,

hence the pressure in the accelerator and the loss of the negative ions by stripping (neutralisation) as they travel through the accelerator. However, all ion sources exhibit a reduced negative ion yield when the filling pressure falls below some value, where the 'filling' pressure is the pressure measured without any discharge in the source, at room temperature. Although this value is ≈ 0.18 Pa in the Kamaboko III source (which is a model of the ITER reference source), the value is as yet unknown for the ITER source and 0.3 Pa is taken as a conservative value. Thus for ITER relevant negative ion beam sources, the value of the gas flow rate through the arc chamber is defined as the gas flow rate providing a filling pressure of 0.3 Pa. This gas flow rate is kept constant during beam source operation. Calculations give values of the gas flow rate into the ITER source of 6.9 Pa m^3 s^{-1} (when operated with a SINGAP accelerator, in H$_2$) to 3.6 Pa m^3 s^{-1} (when operated with a MAMuG accelerator, D$_2$ operation) [8]. As the total area of the apertures in the PG of the ITER source is 1970 cm^2, the particle fluxes are 8.3×10^{17} and 4.6×10^{17} molecules/(s*cm^2) or 74 and 132 equivalent mA cm^{-2}.

2.2. Cs flux

In the ITER neutral beam injector design it was assumed that the filament's lifetime would allow 200 h of operation before they needed to be replaced [9, 10]. Based on experience from short pulse operation, 10 g of Cs should suffice for 200 h of operation, and therefore it is planned to equip each ion source with two ovens, each containing 10 g of Cs. After 200 h of operation, all 72 filaments would be replaced, and the Cs oven(s) would be changed, and, if necessary, Cs would be cleaned off polluted surfaces in the accelerator. These are complicated operations as the ITER injectors will be highly activated and all maintenance will have to be carried out by remote.

It had been assumed that Cs was lost during operation through the extraction apertures. Cs in the ion source has been measured to be >99.9% ionized during operation [11], and Cs$^+$ cannot escape the arc chamber due to the electric field in the extraction gap. Of course the remnant neutral Cs will be lost through the apertures during operation, but, more importantly, Cs will, in principle, be lost due to evaporation from the arc chamber walls between pulses. For example, at 25 °C the Cs saturated flux density (from a pure Cs surface)
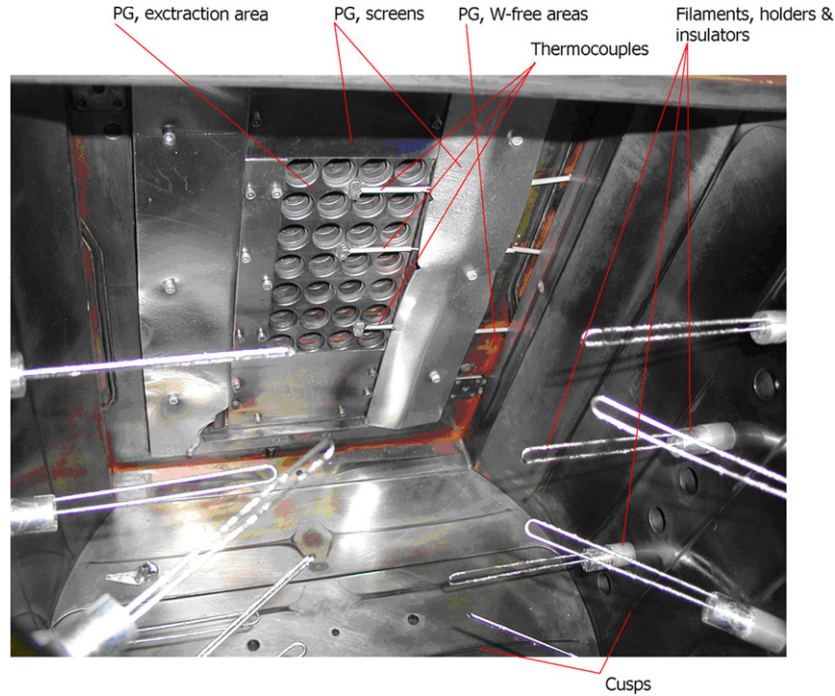
Figure 1. View of the Kamaboko III arc chamber just after opening to the atmosphere following $\approx 10^4$ s of caesiated discharges at 45 kW. The uncooled side screens (or masks) were damaged during long pulse operation (see figure 3).

is 2.8×10^{14} cm^{-2} s^{-1} and it is calculated that 10 g of Cs will leave through the aperture area of 1970 cm^2 in one day plus one night.

In recent MANTIS Kamaboko III campaigns (August 2004 and April 2005), several key spectral emission lines were monitored [11]. It was found that stable and reproducible beam extraction is achieved when the arc chamber is continuously fed with Cs at a flow rate of ≈ 2.5 mg min^{-1} (1.9×10^{17} Cs atoms s^{-1}). With fluxes 10–20% lower or higher the extracted negative ion beam decreased. This Cs flow rate corresponds to an average of 4.6×10^{13} Cs atoms s^{-1} cm^{-2} to the ≈ 5000 cm^2 surface of the arc chamber plus PG. This rate is sufficient to re-establish one Cs monolayer in the arc chamber in 100 s, counteracting the co-adsorption of W evaporated from the filaments (see section 2.3 below).

2.3. Tungsten flux

Tungsten (W) appears in the arc chamber via evaporation from the filaments. In comparison with Cs, which comes from the oven or is re-evaporated from the walls, tungsten appears directly in the main volume of the ion source. From spectroscopic measurements (see the next section) made along lines of sight perpendicular to the PG surface, and along those parallel to the PG, the density of W was found to be rather low, 1.3×10^8 and 0.5×10^8 cm^{-3}, respectively. This is, however, consistent with an estimation based on an ionization balance that any tungsten in the source will be highly ionised. The ionization energy of W is 7.86 eV, and it is calculated that in a plasma with an electron temperature ≈ 3 eV and an electron density of 5×10^{12} cm^{-3}, the W is 99% ionised. Also there is indirect but clear evidence that tungsten is present in the plasma mainly as W$^+$ ions in that there are surfaces such as the periphery of the PG, which remain copper coloured after

most other surfaces have become grey, i.e. tungsten coloured, see figure 1. Such areas are all 'protected' by magnetic fields, which would hinder the flow of W$^+$ to the surfaces, but which would have no effect on neutral W. Hence it can be deduced that W is highly ionised in the Kamaboko III plasma. Therefore, like Cs, it cannot leave the arc chamber during negative ion beam extraction. It is observed that in pure hydrogen operation, i.e. without Cs in the source, the evaporated W atoms normally stick very firmly to clean metal surfaces, such as the source walls. This prevents from W re-evaporating from such surfaces and escaping between pulses. When the source is caesiated, the W is only loosely bound to the source walls, but it nevertheless remains in the ion source, see below.

A simple assessment of the W flux from the filaments into the source is not reliable, because the heating of the filaments is not uniform and this leads to a complicated variation in temperature along the filament and hence in the local W evaporation rate. Therefore a numerical simulation of the filament operation has been performed, and some results are given below.

Following the last campaign, the total decrease in the mass of the 12 filaments used was measured and it was found that 1.50 g of W had been lost from the filaments during a total plasma operation time of 10^4 s. This gives an average value of W flux (in any form) in the arc chamber as 5.3×10^{17} atom s^{-1}. It is to be noted that this is comparable with the Cs flux given above.

3. Results of experiments and calculations

3.1. Spectroscopic results

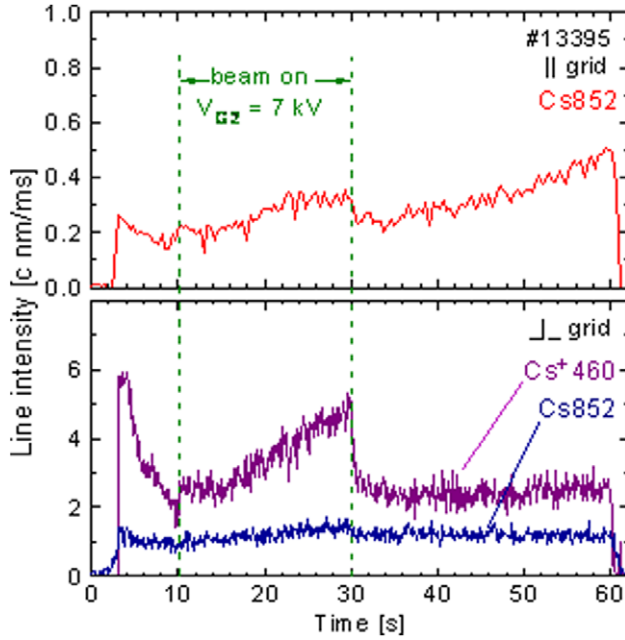In addition to the diagnostics usually applied on MANTIS on-line spectroscopic monitoring and measurements were also

Figure 2. Spectroscopic data taken during arc operation (3–60 s) and beam extraction (10–30 s). Data measured along LOS$_\parallel$ for atomic Cs852 line and along LOS$_\perp$ for Cs852 and the ion line, Cs$^+$460. The Cs$^+$ line intensity increases at $t = 10$ s when the ion extraction ($V_{G2} \approx 7$ kV) starts and falls at the same time as when extraction stops ($t = 30$ s).
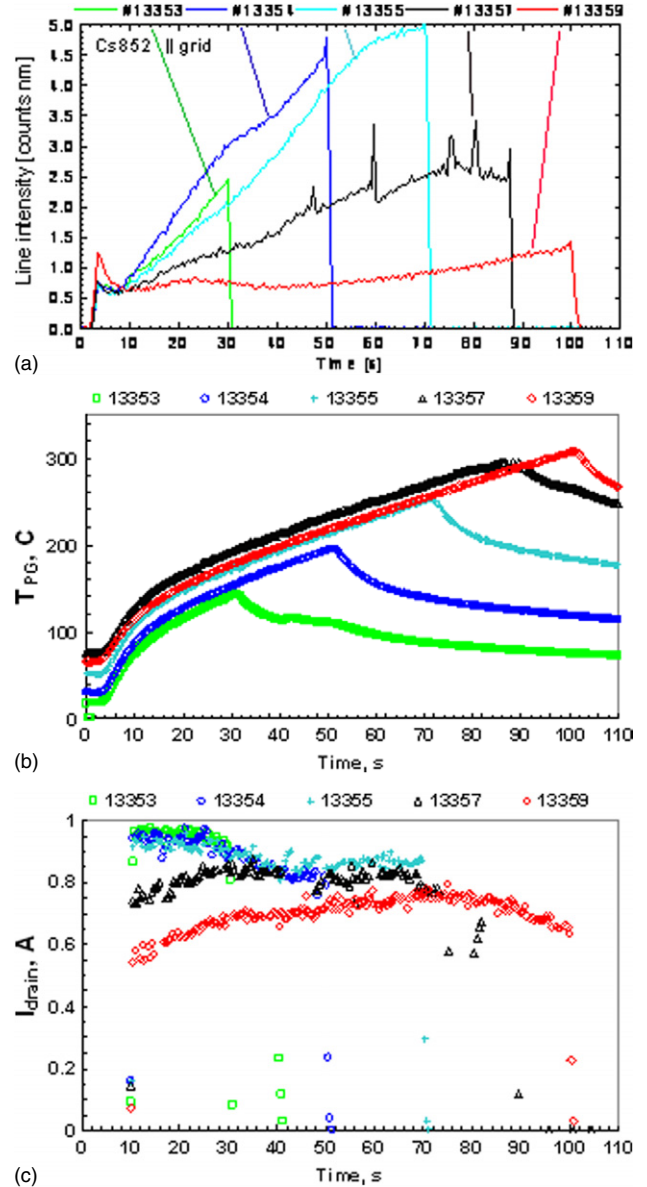

Figure 3. Cs evaporation from the PG. For consecutive shots, the top graph shows the intensity of the atomic Cs852 nm line, the middle graph the PG temperature and the lower graph I_{drain}. For all shots the arc starts at 3 s, the beam extraction at 10 s. The shots stop at 30 s (#13353), 50 s (#13354), 70 s (#13355), 85 s (#13357) and 100 s (#13359).

performed. Detailed results require further study and they will be published at a later time. Here they are used only to the extent required for the subject under consideration. The spectroscopic data were acquired using four different spectrometers coupled to the source observation ports by mean of optical fibres. Two lines of sight (LOS) were used: one was the vertically mounted parallel to the plasma grid at 17 mm from its surface (LOS$_\parallel$); the other one looked almost perpendicular at the PG surface from the rear of the ion source (LOS$_\perp$). The light collected along each LOS was split into three parts, to feed three spectrometers at the same time.

By alternating the connections between spectrometers and the LOSs, comprehensive measurements of hydrogen lines, Cs lines, W atom lines and lines of possible impurities were obtained.

It was found that in certain conditions increases in the Cs and Cs$^+$ light were measured, in particular, when ions were extracted from the ion source and accelerated to form beams, see figure 2. The increased Cs signal was dependent on the beam-on time and the increase was similar to, or higher than, the stable level before ion extraction. The signal reduced promptly when ion extraction stopped.

The reason for this phenomenon is not known. Backstreaming positive hydrogen ions would not sputter Cs efficiently from the source walls, so this seems an unlikely possibility. It has been suggested Cs$^+$ created in the accelerator is back accelerated into the ion source, as Cs$^+$ with energies of ≈ 7 keV (7 kV was the extraction voltage used) could efficiently sputter Cs accumulated on the back wall of the arc chamber and explain the observed increase in the Cs$^+$ light, but this hypothesis has yet to be tested.

Cs evaporation from the PG was studied in an attempt to correlate this with the PG temperature effect. The results are shown in figure 3. The Cs flow from the oven was switched off, and after shot #13353 the water cooling of the PG was removed. In subsequent shots the pulse duration was increased shot-by-shot in order to reach higher PG temperatures. The Cs852 line intensity was measured along with other parameters, including the PG temperature and the accelerated negative ion current (I_{drain}).

In shot 13354, just after the cooling was switched off, the PG temperature is higher than in previous shots, and the atomic Cs852 line intensity increased substantially. In shot 13355 the Cs852 light remained high, but despite the continued increase in the PG temperature (see shot 13357) the intensity fell and

in subsequent shots (e.g. shot 13359) there is little change in intensity with time in the pulse. It is supposed that the caesium light observed along the $\text{LOS}_{\parallel}$ comes from Cs evaporated from the PG, which should increase as the PG temperature increases. The eventual decrease in the signal from shot to shot indicates that Cs evaporation from the grid has dropped to negligible levels, due either to a decrease in Cs coverage to $\theta_{Cs} \leqslant 1$, or to coverage of the Cs by W. The behaviour of the accelerated negative ion current is difficult to interpret as the Cs on the grid would have been covered progressively with W.

3.2. Analysis of the surface coverage

Following a campaign with Cs in the ion source, the source was opened and the bulk of the Cs that had been injected was found to be still inside the arc chamber. On opening the source, the surface of the arc chamber was covered in what looked like a grey layer, which was quite thick, particularly in the cusp areas. There was no visible indication of Cs on surfaces not facing the arc chamber such as under the masks on the PG or in the thin gap between the PG flange and the arc chamber body. After exposure to air for some hours the appearance of the surface changed significantly and much of the surface was covered, unevenly, by a pale green layer.

To define the composition of the surface layers, samples of the coverage from three representative areas were collected, see figure 1.

- The hot central part of the frame cooled plasma grid, around the extraction apertures.
- The cooled frame of the PG.
- The rest of the arc chamber surface.

The samples were mechanically collected using clean cloth and fixed amounts of water. The samples were then filtered through standard coffee filters. When the filters were dry, an insoluble grey substance was left, which is presumed to be W, which had mass of 6.2 g, 8.8% of the initial mass of the 12 filaments.

A following comprehensive analysis of the filtered water samples was performed in the Laboratory of Radiochemical and Chemical Analysis at the CEA, Cadarache. The analysis gave the physical content (absolute and percentage) of soluble substances in water and the content of the sediment in each sample. The following techniques have been used (the name of devices used are given in parentheses): inductively coupled plasma mass spectrometry (PERKIN ELMER ELAN 6000), inductively coupled plasma atomic emission spectrometry (VARIAN VISTA PRO), Wavelength dispersive x-ray fluorescence (PHILIPS PW1404) and Microwave digester (MILESTONE MLS 1200 mega).

The data could then be easily converted to surface concentrations. These analyses do not identify the chemical composition, which means, for example, that the presence of CsH on the surface is not established. This could be important if such a chemical bonding of Cs plays a significant role in trapping of Cs on surfaces. The results are shown in table 1.

Comments on these results.

- Almost all the injected Cs was found in the arc chamber.

- All surfaces, including the PG extraction area, were covered by thousands of monolayers of Cs and W in comparable amounts (one monolayer is $\approx 5 \times 10^{14}$ at cm^{-2}). Other components were found in the range of 8–10%.
- The amount of Cu and particularly Ca found was unexpectedly large. A possible reason for the presence of Cu in samples may be the physical removal of Cu from the surfaces of the arc chamber and PG during the washing with brush and water and/or sputtering during arc operation. In the latter case the role of Cu co-deposition could be similar to that of W co-deposition, which, it is suggested, restricts Cs evaporation from the walls. The Ca in the samples was probably present in the water used for the cleaning of the source, which was ordinary tap water.
- Mo was found in amounts proportional to that existing in the W filament wire.
- Fe and Al could be sputtered from the thermocouple sheaths and filament insulators that are exposed to the plasma, see figure 1.

Note that the density of the deposit on the extraction area was calculated without taking into account the surface of the apertures. If the material flows through the apertures (i.e. if it is produced whilst ions are being extracted and it is not ionised), then $\approx 22\%$ of those materials will have been lost from the ion source.

The main conclusions from this analysis are the following.

- The plasma grid coverage is a multi-layer composition of Cs, W and other metals. This composition is far from the ideal situation, which is assumed to be a Cs coverage of sub-monolayer thickness on a clean metallic substrate.
- The bulk of Cs did not leave arc chamber but it is 'blocked' on the walls and does not take part in negative ion generation at the PG.

3.3. W evaporation from filaments

A numerical model of the filament, which is directly heated by AC-current on MANTIS, has been developed in order to study the W evaporation process from the filaments. (For DC heated filament operation experimental measurements and calculations were done in Japan in JAEA [12] and NIFS [13].) A better understanding of the evaporation of W could lead to changes in the filament design, e.g. the use of larger diameter filaments, or changes in the way the filament current is regulated, which could lead to lower W evaporation and increases in the life time of the filaments. The model divides the filaments into many sections and includes the following heating/cooling processes, that define the local steady-state operation of each section of the filament.

- Ohmic heating by the AC current from the filament power supply.
- Direct heating from positive ions.
- Direct heating by radiation from other filaments and the plasma.
- Ohmic heating from the fraction of the arc current flowing through the filament section.
- Radiation cooling.

- Cooling by electron emission.
- Cooling by conduction to the filaments holders.

The resistivity, emissivity, electron emission, thermal conductivity, etc of W were input as temperature-dependent values, taken from [14]. The rate of evaporation of W as a function of temperature was taken from [15]. The model included the feedback circuit which allows the arc current to be determined by varying the filament power, which also allows independent control of the (average) anode to cathode voltage.

In the model, the total arc current per filament (the sum of the current of incident positive ions and emitted electrons) was fixed by increasing or reducing the current from the filament power supply in order to get the required electron emission from the filament at the predefined density of positive ions falling in the plasma, which determines the positive ion current to the filament.

An example of a result, calculated for the MANTIS filaments (1.5 mm in diameter and 170 mm length, 50 Hz ac filament power supply), is given in figure 4. It is appropriate to mention here that the total W flux before plasma ignition, assuming a filament temperature 2800 K, is 3.5×10^{16} atoms/s, that is, 5.5 times less than calculated for plasma operation (shown in the figure legend). In the code the arc starts as soon as the filaments reach the pre-set temperature, 2800 K in this case. In actual operation the arc is typically initiated some seconds after this point. As noted above, the evaporated W is highly ionised during the discharge and cannot easily reach some parts of the ion source which are protected by magnetic fields, nor escape into the accelerator. However during the 1–2 s when the filaments are hot (2800 K) but there is no discharge, W evaporated from the filaments will be deposited on all surfaces of the arc chamber in direct line of sight of the filaments, including the PG and some parts of the extraction grid and other downstream surfaces.

The initial heating of the filaments, as described above, should ensure that the filaments are Cs free at arc initiation. Thereafter the W filaments work in the presence of a Cs flux to their surface, mainly as Cs^+. Now the filament operating temperature ($\geqslant 2800$ K) is well above the minimum temperature for Cs surface ionisation [16], so any Cs leaving the filament will leave as an ion. However, when the source plasma is present, any Cs^+ leaving the surface cannot overcome the plasma sheath potential and it will return to the surface, i.e. any Cs arriving at the filament will be trapped on the filament. However, Amersfoort [17] has shown that under these conditions strong self-sputtering, by Cs^+ from the plasma accelerated in plasma sheath, onto the filament surface, results in a Cs coverage of the W surface which is not more than 20%.

Accumulation of Cs on the W surface could change the work-function value of the surface and therefore its electron emission. No decrease of W work function value caused by this phenomenon was taken into account in the present model. This is justified as (a) the initial heating of the filament, prior to establishing the arc, to $\geqslant 2800$ K will evaporate essentially all the Cs from the filaments and (b) even if Cs is initially present, the coverage will be $<20\%$ of a monolayer, and the change in work function will be small.

The calculations presented below were done for the Kamaboko III source operation with various number of
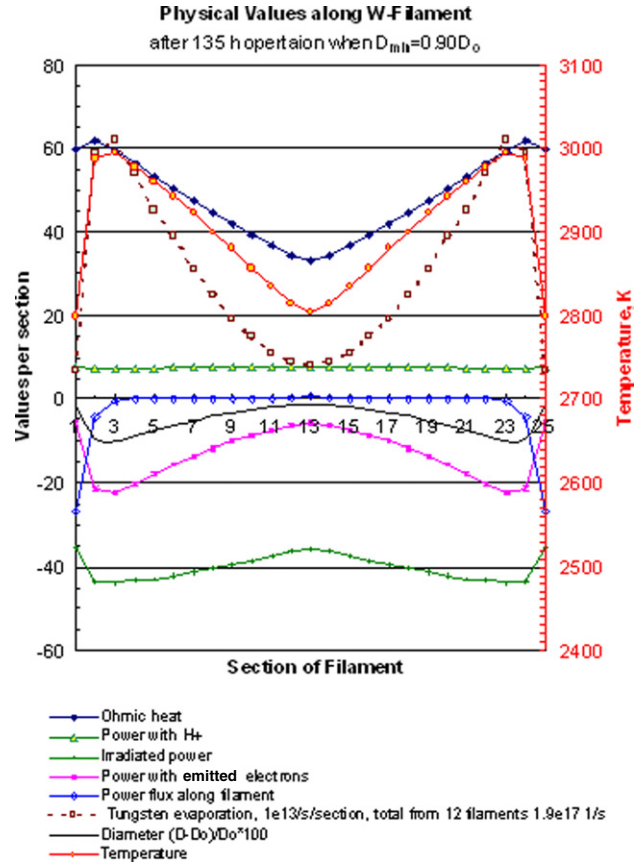

Figure 4. ac heated MANTIS filament during operation. The main contributors to the power equilibrium are shown in the legend. Heat sources are positive; heat sinks are negative. The local diameter and temperature are also shown.

filaments: from 12 (the standard number for Kamaboko III source) to 6. With half the number of filaments (assuming the same arc power) the calculated evaporation increased by more than a factor of 3. The calculations show that the total flux of W cannot be reduced significantly by operating with, say, twice as many filaments, or with filaments with a diameter twice as big, because of the relatively weak dependence of emission/evaporation ratio with temperature, see figure 5. We note that in principle we would like the flux of tungsten to the PG to be much less than that of Cs.

The calculated filament lifetime (taken as the time to reach a local minimum diameter $\approx 90\%$ of the initial diameter) for 12 filament operations (130 h) is a factor of 5 times longer than for 6 filament operation. A similar increase is calculated for filaments with a larger diameter. So for the MANTIS case using 2.0 mm filaments would increase the lifetime by ≈ 310 h. It is clear from these calculations that the filament lifetime due to evaporation increases with the filament diameter and larger filament diameters should be considered for the ITER source, e.g. 2.5 mm instead of the 2 mm proposed will increase life time from 350 h to 460 h (for standard ITER operation at 790 kW of arc power, 72 filaments). Preliminary studies show no problems in using such large diameter filaments, e.g. there is no limitation in electron emission by the self magnetic from the required increased heating current.

To a first approximation the negative ion yield is proportional to the arc power [18], so that operation at a
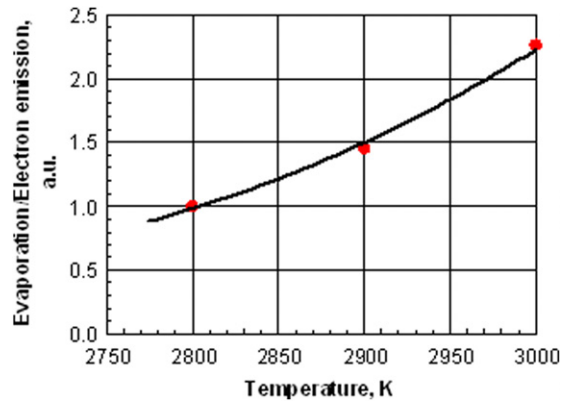
Figure 5. Change of W evaporation/electron emission ratio with filament temperature (the ratio is normalized to unity at 2800 K). Operation with lower temperature (more filaments or larger diameter of filaments) reduces the filament evaporation and extends the filament life.
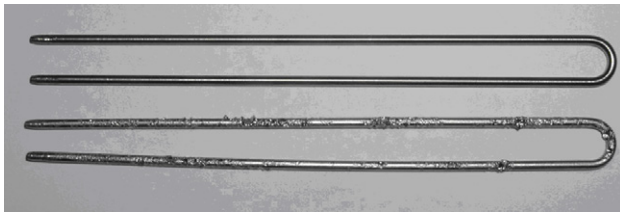

Figure 6. The MANTIS Kamaboko III tungsten filaments (1.50 mm diameter, 170 mm length): the new above, and the used after 10^4 s of plasma operation. 0.13 g of the initial 6.26 g was lost during operation.

higher anode to cathode voltage requires less current for the same extracted negative ion current, hence a lower filament temperature. Consequently less W evaporation was calculated for a plasma operation with higher anode–cathode voltage for the Kamaboko III ion source. With 12 filaments, changing the anode to cathode voltage from 50 V to 70 V decreases the evaporation to 2.2×10^{17} from 3.8×10^{17} atoms s^{-1} and increases the life time to 235 h.

Unfortunately it appears that evaporation may not be, at present, the most critical factor in determining the filament life. Figure 6 shows a new filament and a filament after 10^4 s of plasma operation. Craters are randomly distributed along the surface of the used filament. In some places the size of these craters (diameter, depth) is comparable with the filament diameter. The reason for this phenomenon is still not clear. Possible causes are uni-polar arcs to the plasma, arcs to the source walls or sputtering by Cs$^+$ or W$^+$. Although each filament is protected from over-currents, small local arcs to the source walls, or uni-polar arcs to the plasma, could go unnoticed. The hypothesis that Cs$^+$ or W$^+$ sputtering causes the craters is supported by the observation that the craters are more numerous when operating with Cs. Also, it has been measured that the arc current varies from filament to filament at least by 10–20%, which will cause variations in filaments evaporation lifetime within the installed filaments. The reason for this variation has not yet been identified. It could be due to the Ohmic contacts with the filament supports or variations in the filament emissivity.

4. Conclusions and discussion

During long pulse operation of the Kamaboko III beam source on the MANTIS test bed at the DRFC, CEA, Cadarache, a considerable amount of Cs has be continuously injected to keep the accelerated negative ion current high. The result is a very high Cs 'consumption' rate. Additionally only a small 'PG temperature effect' is observed.

Inspection of the arc chamber surfaces after experimental campaigns and subsequent chemical analyses have shown that practically all the injected Cs was still inside the arc chamber in a mixture of tungsten and a few other metals. Cs and W are found in comparable amounts ($\approx$3 g of Cs and 1.5 g of W).

It is suggested that the need for high, continuous Cs injection arises because the Cs is 'blocked' on the source walls in a loosely bound matrix of Cs and W evaporated from the filaments [3, 7]. This mixture seems to inhibit the evaporation of Cs, as is evidenced by the low loss of Cs from the ion source after long periods of operation. The lack of Cs evaporation from the walls would inhibit the replenishment of the Cs layer on the PG where it is considered that the extracted negative ions are produced. This effect is much worse in long pulse operation where the total evaporated W becomes comparable to the injected amount of Cs.

The PG temperature effect is expected with a pure W surface coated by Cs. However it is clear that no such surface exists during the long pulse operation of the Kamaboko III ion source. The PG surface is coated by a Cs W mixture. As is the case for the source walls, the evaporation of Cs from this mixture is lower than that of pure Cs on a W surface, hence both the Cs flux to the PG and the evaporation from the PG are different from those pertaining to the short pulse operation, and it is not unexpected that the PG temperature effect is not the same for the same temperature range. Unfortunately the attempt to observe the Cs evaporation from the PG by increasing its temperature whilst monitoring the Cs emission in front of the PG was inconclusive.

The filament lifetime in the Kamaboko III source and in the ITER reference design of negative ion source will be limited by W evaporation from the filaments in the absence of other factors. In the case of the Kamaboko III source many craters are observed on the surface of the filaments, which might limit the filament lifetime. However the measured decrease in the mass of 12 filaments is in agreement with calculations of tungsten loss by evaporation alone, suggesting that this might not be the case. (The craters may simply be a redistribution of the W, not necessarily a local loss of W.)

It is suggested that using larger diameter filaments could increase the filament life in the ITER reference ion source.

If the adverse effects of long pulse operation (increased Cs consumption and reduced PG temperature effect) are a result of W evaporation, then these can be avoided by using low temperature emitters, such as thoriated tungsten or LaB$_6$. Lower temperature emitters could also remove the possible problem of the observed craters if the materials operate far from their melting point, so that more energy is needed to cause the local melting necessary to form the craters.

References

[1] Van Wunnik J.N.M. *et al* 1983 The scattering of hydrogen from a cesiated tungsten surface *Surf. Sci.* **131** 17–33

[2] Okumura Y., Hanada M., Inoue T., Kojima H., Matsuda Y., Ohara Y., Seki M. and Watanabe K. 1990 Caesium mixing in the multi-ampere volume H⁻ ion source *5th Int. Symp. on the Production and Neutralization of Negative Ions and Beams (Brookhaven National Laboratory, Upton, NY, USA) AIP Conf. Proc.* **210** 169–83

[3] Fumelli M., Jequier F., Pame1a J. and Simonin A. 1995 Negative ion production with the PAGODA source *Fusion Eng. Des.* **26** 463–72

[4] Trainham R., Jacquot C., Riz D., Simonin A., Miyamoto K., Fujiwara Y. and Okumura Y. 1998 Negative ion sources for neutral beam injection into fusion machines *Rev. Sci. Instrum.* **69** 926–28

[5] Boilson D., de Ecsh H.P.L., Hemsworth R.S., Kashiwagi M., Massmann P. and Svensson L. 2002 Long pulse operation of the Kamaboko III negative ion source *Rev. Sci. Instrum.* **73** 1093–5

[6] Hemsworth R.S., Boilson D., de Esch H.P.L., Krylov A., Massmann P. and Svensson L. 2006 Some lessons from long pulse operation of negative ion source and accelerators *Nucl. Fusion* **46** 1–11

[7] Belchenko Yu.I. *et al* 2002 Negative ion production in multicusp sources *Rev. Sci. Instrum.* **73** 1746–51

[8] Krylov A. and Hemsworth R.S. 2006 Gas flow and related beam losses in the ITER neutral beam injector *Fusion Eng. Des.* at press

[9] Inoue T. *et al* 2001 Design of neutral beam system for ITER-FEAT *Fus. Eng. Des.* **56-57** 517–21

[10] 2001 Neutral Beam Heating & Current Drive (NBH&CD) *System ITER Design Description Document* DDD 5.3 (http://www.naka.jaea.go.jp/ITER/FDR)

[11] Fantz U., Falter H. D., Franzen P., Speth E., Hemsworth R.S., Boilson D. and Krylov A. 2006 Plasma diagnostic tools for optimizing negative hydrogen ion sources *Rev. Sci. Instrum.* **77** 03A516 1–4

[12] Miyamoto N., Fujiwara Y., Miyamoto K. and Okumura Y. 2000 Steady state operation of an ampere-class hydrogen negative ions source *Rev. Sci. Instrum.* **71** 738–40

[13] Oka Y *et al* 2004 Studies of H- source for large helical device-neutral beam injector *Rev. Sci. Instrum.* **75** 1803–8

[14] Handbook of Chemistry and Physics 1981-1982 62nd edn ed R.C. Weast and M.J. Astle (Boca Raton, FL: CRC Press)

[15] Reiman A. L. 1938 The evaporation of atoms, ions and electrons from tungsten *Phil. Mag.* **215** 834–48

[16] Taylor J.B. and Langmuir I. 1933 The evaporation of atoms, ions and electrons from caesium films on tungsten *Phys. Rev.* **44** 423

[17] van Amersfoort P.W. 1985 Formation of negative ions on metallic surface *PhD Theses* FOM-Institute for Atomic and Molecular Physics, Amsterdam 71

[18] Boilson D., Ellingboe A.R., Faulkner R., Hemsworth R.S., de Esch H.P.L., Krylov A., Massmann P. and Svensson L. 2005 Negative ion yield in long pulse operation of the KAMABOKO III source *Fusion Eng. Des.* **74** 295–8